Natural Hazards (2006) 38: 355–374
DOI 10.1007/s11069-005-1921-y

A Quantitative Assessment of the Human and Economic Hazard from Impact-generated Tsunami

STEVEN R. CHESLEY[1,★] and STEVEN N. WARD[2]
[1]*Jet Propulsion Laboratory, California Institute of Technology, Pasadena, CA 91109, USA;* [2]*Institute of Geophysics and Planetary Physics, University of California, Santa Cruz, CA 95064, USA*

(Received: 17 October 2003; accepted: 30 July 2005)

Abstract. In this article, we assess the human and economic hazard posed by tsunami waves generated from impacts of sub-2 km diameter asteroids. Annually, on average, 182(+197/−123) people will be affected by impact-induced waves with a corresponding infrastructure loss of $18(+20/−12)M/y. Half of the tsunami hazard stems from impactors with diameters less than 300 m. One near Earth asteroid will survive atmospheric transit and strike somewhere into Earth's oceans every 5880 years, on average. In the mean generic scenario, the tsunami from the impact affects 1.1 million people and destroys $110B of infrastructure.

Key words: Asteroid, Impact, Tsunami

1. Background

Currently, telescopes under the Spaceguard Survey routinely search for and track Near Earth Asteroids (NEAs) 1 km diameter and larger. Earth impact of these bodies likely occasion catastrophes on hemispheric to global scales. Recently though, the United States National Research Council has twice recommended the construction of a Large-aperture Synoptic Survey Telescope (LSST) designed in part for detecting and tracking NEAs as small as 300 m diameter (NRC, 2001, 2002). Among the rationales for the $150M LSST would be its role in mitigating impact-related hazards of sub-km-size asteroids. Because oceans cover two-thirds of the Earth's surface and knowing that water waves can transmit energy to great distance, it has been thought that of all the risks related to sub-km-size asteroid strikes, impact-generated tsunami loom largest.

Just how compelling is the impact tsunami hazard? The importance of addressing this question has been specifically cited as a research priority by

★ Author for correspondence: E-mail: steve.chesley@jpl.nasa.gov

the international Organization for Economic Cooperation and Development (2003). Moreover, on December 26, 2004 two events spotlighted tsunami hazard on the world stage. First, was the Sumatra–Andaman earthquake whose spawned tsunami killed about 200,000 people (Lay *et al.*, 2005). Second was the discovery of asteroid 2004 MN4 (Schweickart, 2005) which, on that day, was calculated to have a 1-in-37 chance of striking the Earth in 2029 (Figure 1). Quantifying the human and economic hazards of impact tsunami from asteroids like 2004 MN4 depends on three principal ingredients: (a) the frequency and diameter of asteroids that strike Earth's oceans; (b) the amplitude of impact-generated water

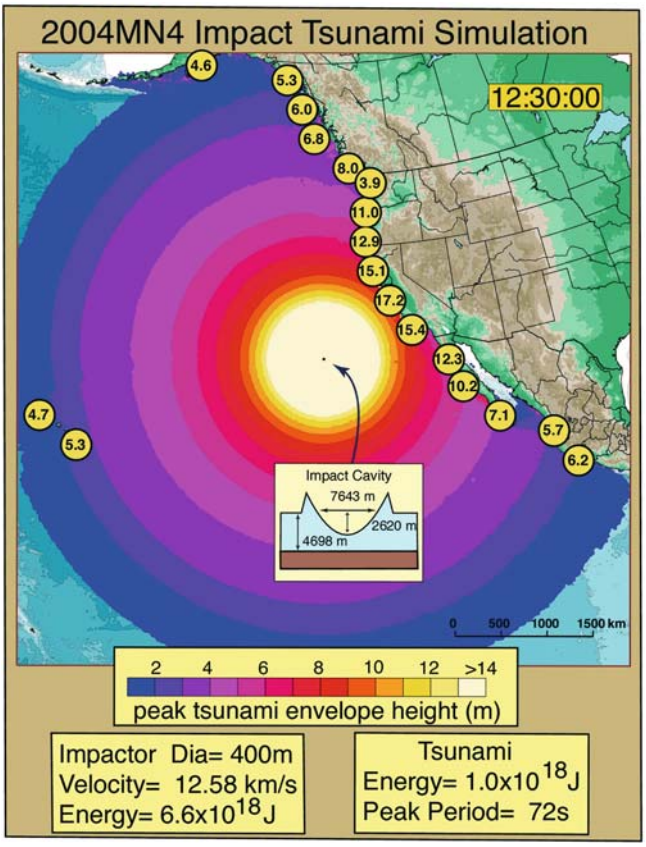

Figure 1. Simulation of the impact tsunami from asteroid 2004 MN4. At 400 m diameter, 2004 MN4 is representative of the asteroids of interest in this article. The colors show peak tsunami height versus distance from the impact site 1000 km west of the North America coast. Numbers within the yellow dots show estimated run-up in meters. Note the initial cavity size, the spreading of the waves, their decay with distance, their growth in shallow water and their eventual run-up on shore. These effects are incorporated quantitatively in Equations (2)–(7).

waves and their evolution during propagation; and (c) the near shore distribution of people and infrastructure exposed to flooding. Fixing each element is fraught with uncertainties; however, diverse research in tsunami mechanics (Ward and Asphaug, 2000) and coastal population distribution (Small *et al.*, 2000) has developed to where we can lay down the steps involved in hazard estimation and make the first quantitative evaluation of impact tsunami risk.

2. Impact Tsunami Statistics Model

2.1. ASTEROID FLUX RATE

Fundamentally, the frequency of impact tsunami hinges on the flux of asteroids into the world's oceans. Impact flux, a strong function of asteroid diameter, is modeled here by a cosine-tapered power law

$$f_{>}(D_{\mathrm{I}}) = 20\,\mathrm{yr}^{-1}(D_{\mathrm{I}}/1\,\mathrm{m})^{-7/3} \quad D_{\mathrm{I}} > 200\,\mathrm{m} \tag{1a}$$

$$f_{>}(D_{\mathrm{I}}) = 2\,\mathrm{yr}^{-1}(200\,\mathrm{m}/1\,\mathrm{m})^{-7/3} + f_{\mathrm{atmos}}(D_{\mathrm{I}}); \quad D_{\mathrm{I}} < 200\,\mathrm{m} \tag{1b}$$

where

$$f_{\mathrm{atmos}}(D_{\mathrm{I}}) = \frac{70}{3\,\mathrm{yr\,m}} \int_{\max[D_{\mathrm{I}},60\mathrm{m}]}^{200\mathrm{m}} \left(1 - \cos\frac{\pi(D_{\mathrm{I}} - 60\,\mathrm{m})}{(200\,\mathrm{m} - 60\,\mathrm{m})}\right)\left(\frac{D_{\mathrm{I}}}{1\,\mathrm{m}}\right)^{-10/3} \mathrm{d}D_{\mathrm{I}}.$$

In (1) $f_{>}(D_{\mathrm{I}})$ denotes the mean impact frequency of stony objects larger than diameter D_{I} anywhere on Earth (Figure 2). Flux (1) reflects a 5-fold decrease from that used by Ward and Asphaug (2000). The decrease brings rates better into line with recent estimates (Brown *et al.*, 2002 and references therein). Of course, only 2/3 of the total flux falls into water. Also, the Earth's atmosphere shields the surface from small asteroids so impact rate (1b) begins to taper down for impactors with $D_{\mathrm{I}} < 200$ m, flattening out almost completely for stony asteroids with $D_{\mathrm{I}} < 60$ m. (Iron asteroids much smaller than 60 m survive atmospheric transit, but compared to the numbers of stony asteroids, irons comprise a tiny fraction.) The transition from "unshielded" to "shielded" is gradual because impactor velocity, strength, and impact angle contribute to their survivability as well as diameter. The mean recurrence interval for any impact event at the Earth's surface is 3330 years. Let's suppose that the bolide of interest for LSST has $D_{\mathrm{I}} = 300$ m. Equation (1) predicts one Earth impact of this size or greater every 30,000 years.

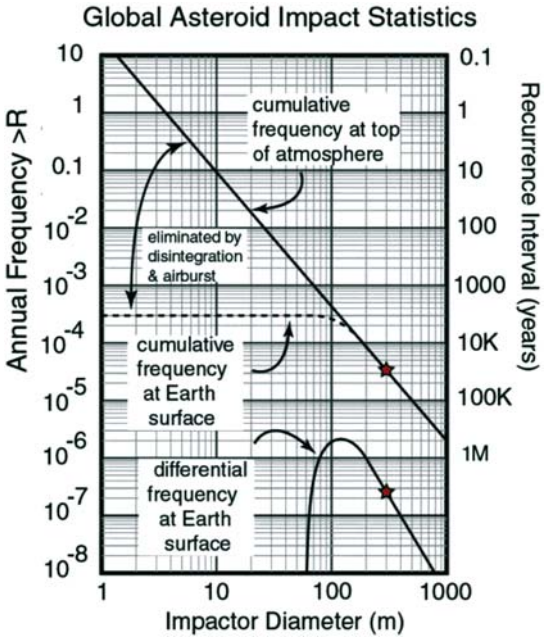

Figure 2. Cumulative annual impact frequency $f_{>}(D_{\mathrm{I}})$ for stony NEAs with diameters larger than D_{I} at the top of the atmosphere (upper solid curve) and at the Earth's surface (dashed curve). Atmospheric shielding accounts for the difference in the fluxes. Lower solid curve shows the differential flux rate $\partial f_{>}(D_{\mathrm{I}})/\partial D_{\mathrm{I}}$. Stars are for the 300 m bolide of interest.

2.2. INITIAL CAVITY FORMATION

The size of the transient water cavity created during an impact dictates the size of the spawned tsunami. Transient cavity size depends on impactor kinetic energy through its diameter, bulk density ρ_{I}, and impact velocity V_{I}, together with the efficiency ε_{I} of energy transfer to the water. For $\rho_{\mathrm{I}} = 3$ gm/cm^3, $V_{\mathrm{I}} = 20$ km/s, and $\varepsilon_{\mathrm{I}} = 0.15$, Ward and Asphaug (2002) approximate transient cavity diameter d_{c} and depth D_{c} by

$$d_{\mathrm{c}}(D_{\mathrm{I}}) = 117\,\mathrm{m}(D_{\mathrm{I}}/1\,\mathrm{m})^{3/4} \tag{2}$$

and

$$D_{\mathrm{c}}(D_{\mathrm{I}}) = d_{\mathrm{c}}(D_{\mathrm{I}})/3.13, \tag{3}$$

respectively. Striking a deep ocean, our 300 m impactor makes a transient cavity 8.4 km wide and 2.7 km deep (Figure 3). For perspective, the tsunami energy generated from this impact, $(1/12)\pi\rho_{\mathrm{w}} g(D_{\mathrm{c}} d_{\mathrm{c}})^2 = 1.3\times10^{18}$ J exceeds that of the devastating 2004 Sumatra tsunami by a factor of about 300 (Lay *et al.*, 2005).

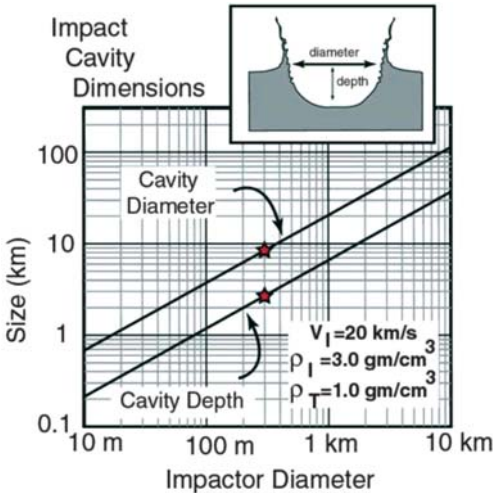

Figure 3. Transient impact cavity sizes as modeled by Equations (2) and (3). Stars are for the 300 m bolide of interest.

2.3. DEEP-WATER WAVE PROPAGATION

The collapse and subsequent oscillation of the impact cavity incite a series of waves that move out from the impact point $\mathbf{r}_0$ and diminish in size, roughly as inverse distance traveled, due to geometrical spreading and frequency dispersion. For a constant depth ocean, Ward and Asphaug (2002) fit the peak tsunami amplitude at point $\mathbf{r}$ by

$$A(\mathbf{r}) = \min[h(\mathbf{r}_0), D_c(D_I)] \left[\frac{1}{1 + 2|\mathbf{r} - \mathbf{r}_0|/d_c(D_I)} \right]^{\psi}$$
$$\psi = 1/2 + 0.575 \exp[-0.0175 d_c(D_I)/h(\mathbf{r}_0)]. \quad (4)$$

If the 300 m asteroid impacts into 5000 m of water, tsunami of 8.2, 4.0, and 2.6 m would reach to 1000, 2000 and 3000 km distance, respectively (Figure 4). Be aware that the largest wave possible in (4) is the smaller of the cavity depth $D_c(D_I)$ given by (3) and the ocean depth at the impact site $h(\mathbf{r}_0)$.

2.4. SHOALING

When tsunami reach shallow water they slow and grow to conserve energy flux.

For the waves of interest, deep water amplitude $A(\mathbf{r})$ from (4) needs to be corrected to a "shoaled amplitude" $A(\mathbf{r}_s)$ by (Dingemans, 1997)

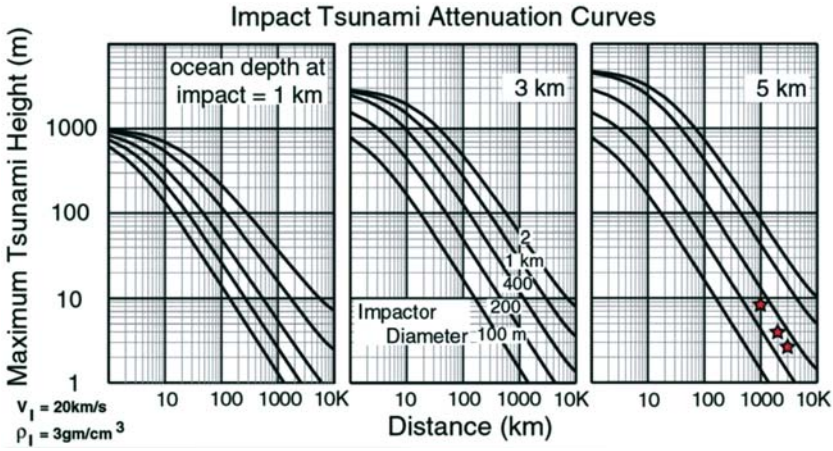

Figure 4. Deep water impact tsunami heights as modeled by Equation (4). Curves represent different impactor sizes. Panels represent different ocean depths at impact. Stars are for the 300 m bolide of interest.

$$A(\mathbf{r}_s) = A(\mathbf{r})\left[\frac{V(\omega_{\max}, h(\mathbf{r}_0))}{V(\omega_{\max}, h(\mathbf{r}_s))}\right]^{1/2}. \tag{5a}$$

Shoaling amplification depends on the ratio of tsunami group velocity V, at the impact-site and the shoaled-site (ocean depth $h(\mathbf{r}_0)$ and $h(\mathbf{r}_s)$, respectively) evaluated at the frequency associated with the peak tsunami strength (see Ward and Asphaug, 2000). A quick approximation to (5a) is

$$A(\mathbf{r}_s) \sim (1/2)A(\mathbf{r})[h(\mathbf{r}_0)/h(\mathbf{r}_s)]^{1/4}. \tag{5b}$$

If $h(\mathbf{r}_s) = 10$ m and $h(\mathbf{r}_0) = 5000$ m, then shoaling increases deep water wave heights (4) by a factor of 2.36. Equation (5) holds only to a critical depth where $A(\mathbf{r}_s) = h(\mathbf{r}_s)$. We call the tsunami amplitude at this point A_{crit}.

2.5. TSUNAMI STATISTICS AT A GENERIC COASTAL SITE

Equations (1)–(5) provide the information to compute a rate density for shoaled tsunami of specified sizes. For some generic site, the frequency of waves >10 m high from bolides $D_I > 300$ m is computed by the double integral

$$\dot{N}_w(A_{\text{crit}}, D_{\min}) = \int_{A_{\text{crit}}=10\,\text{m}}^{\infty} \mathrm{d}A_{\text{crit}} \int_{D_{\min}=300\,\text{m}}^{\infty} \mathrm{d}D_I R_w(A_{\text{crit}}, D_I), \tag{6}$$

where $R_w(A_{crit},D_I)$ is the generic tsunami rate density. Equation (1) gives a global frequency 3.3×10^{-5}/y for $D_I > 300$ m impacts, but a large fraction of these strike land or hit too far away and fail to make the needed wave, so certainly $\dot{N}_w(A_{crit}, D_{min}) < 3.3 \times 10^{-5}$/y. To exceed a 10 m height near shore, (5b) with $A(\mathbf{r}_s) = h(\mathbf{r}_s) = A_{crit} = 10$ m, says that the wave must have deep water amplitude $A(\mathbf{r}) > 10$ m/2.36 = 4.2 m. Equation (4) further dictates that a 300 m bolide has to fall within $D_{crit} = 1900$ km of the generic site to make 4.2 m waves. Farther away and the waves will have weakened too much. The extent of ocean visible within the 1900 km critical distance depends upon how strongly the site bears to the sea – the more laid-open, the higher the rate of inundation. We imagine a generic coastal site with a 180° view (called exposure) over a 6000 km expanse (called reach) of open ocean. Our ocean is generic also; including a sloping 100-km-wide continental shelf that, at its edge, deepens from 200 to 5000 m within 1500 km from shore and then flattens out (Ward and Asphaug, 2000). As seen from this generic site, the ocean visible within 1900 km covers 2.2% of the Earth's surface, so a first guess at the rate of impact tsunami $A_{crit} > 10$ m from bolides $D_I > 300$ m would be

$$\dot{N}_w(A_{crit}, D_{min}) \approx 0.022 \times 3.3 \times 10^{-5}/y = 7 \times 10^{-7}/y$$

The actual computations in this article evaluate integrals (6) directly, use (5a) versus (5b), and take into account that D_{crit} grows with impactor size. Still, the concept ought to be clear that only a fraction of ocean impacts of a given size fall close enough to a generic point to make tsunami of a given size. Figure 5 graphs generic tsunami rate density $R_w(A_{crit}, D_I)$ as a function of critical wave height and impactor diameter. Because (1) predicts far fewer large impacts than small ones, $R_w(A_{crit}, D_I)$ falls-off with increasing bolide size. On the small end, atmospheric shielding causes $R_w(A_{crit}, D_I)$ to decay rapidly for $D_I < 100$ m because few small asteroids reach Earth's surface. As a consequence of these two effects, the most probable impact-generated tsunami have $A_{crit} < 10$ m and derive from asteroids 100–400 m diameter.

3. Tsunami Inundation Model

The number of people affected by a tsunami depends upon how far the beaching wave rises in elevation (the *run-up, R*) and how far the waves surge inland (the *run-in, X*).

3.1. RUN-UP

Wave run-up is complex. For this work we require an easily computed, globally applicable recipe to estimate run-up height R, given a shoaled

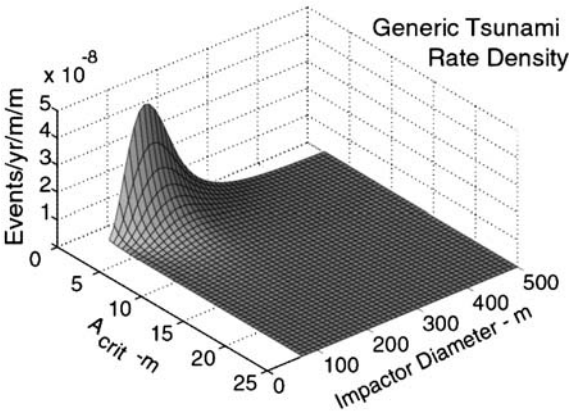

Figure 5. Generic tsunami rate density $R_w(A_{crit},D_I)$ as a function of impactor diameter D_I and critical wave amplitude or run-up height A_{crit}.

wave amplitude offshore. Ward and Asphaug (2003) distilled run-up to its simplest essence in

$$R = A(\mathbf{r}_s)^{4/5} h(\mathbf{r}_s)^{1/5}. \tag{7}$$

Like Equation (5), Equation (7), is based on conservation of wave energy flux (see Appendix). It forecasts run-up height R, from any offshore shallow water position $\mathbf{r}_s$ provided $A(\mathbf{r}_s) < h(\mathbf{r}_s)$. Laboratory experiments on solitary waves (Synolakis, 1987) suggest that (7) works adequately well for both breaking and non-breaking waves over a range of beach slopes. If $A(\mathbf{r}_s) = h(\mathbf{r}_s)$, then $A(\mathbf{r}_s) = A_{crit} = R$ are one and the same.

3.2. RUN-IN

Realistically, the distance that tsunami run inland ought to vary with its height, persistence, and the friction presented to the waves by landforms, vegetation, and structures. Taking a clue from "skin depth" laws for penetration of electromagnetic waves into conductors, we let run-in distance X equal the product of wave velocity at beaching V_b times wave period T

$$X = V_b T. \tag{8}$$

X in (8) equals one wavelength of inland penetration. For wave speed at beaching we use the shallow water formula

$$V_b = \sqrt{gR}, \tag{9}$$

where R is the run-up height known from (7). Asteroid impacts excite tsunami waves of all periods; however, the period T of the largest waves corre-

sponds to the fundamental period of oscillation of the initial transient cavity. For deep water impacts, T grows with transient cavity diameter d_c like

$$T(d_c) \approx 1.2\sqrt{2\pi d_c/g}, \tag{10}$$

where $g = 9.8$ m/s^2. With (2), (10) becomes a function of impactor diameter

$$T(D_I) \approx 10\,\mathrm{s}\,(D_I/1\,\mathrm{m})^{3/8}. \tag{11}$$

The subject 300 m bolide creates peak tsunami waves with $T = 85$ s. Typically, impact tsunami have periods long compared to wind-driven waves ($\sim$10 s) but short compared to tsunami from large earthquakes ($\sim$1000 s). With (9) and (11), run-in distance (8) becomes

$$X(R, D_I) \approx 10\mathrm{s}\sqrt{gR}(D_I/1\mathrm{m})^{3/8}. \tag{12}$$

Waves from our 300-m impactor run-in about 0.8 km when $R = 10$ m. In general, tsunami from sub-km-sized objects can run-in 2–3 km depending upon the distance to impact, hence run-up height (Figure 6). As evidenced in the Indian Ocean in 2004, smaller earthquake tsunami, due to their longer periods, can penetrate much further inland than impact tsunami. According to (8) and (9) a 1000 s period earthquake tsunami with 3 m run-up might run in 5.5 km over flat ground.

4. Human Hazard: The Generic Model

4.1. COASTAL POPULATION STATISTICS

The extent to which global population concentrates in low-lying coastal areas has only recently been carefully characterized (Small *et al.*, 2000). Figure 7 plots the cumulative human population $P_<(D, E)$ living within $D = 100$ km from shore and below $E = 100$ m elevation. We interpolated this detailed $P_<(D, E)$ from Small *et al.*'s (2000) original coarse-sampled data (10 km by 10 m bins) with the additional assumption that no one resides below 2 m elevation.

Clearly, the "population at risk" $N_R(R,D_I)$ from impact-induced tsunami must live below run-up elevation R and within run-in distance X

$$N_R(R, D_I) = P_<(X(R, D_I), R). \tag{13}$$

Globally, about 50 million people (Figure 8) are exposed to the most common tsunami events ($R < 10$ m from 100 m $< D_I <$ 400 m impacts). To find the rate at which those 50 million people *actually become affected* we first multiply (13) by the generic tsunami rate density (Figure 5) to get the rate density of affected population $\dot{N}_A(R, D_I)$ (Figure 9)

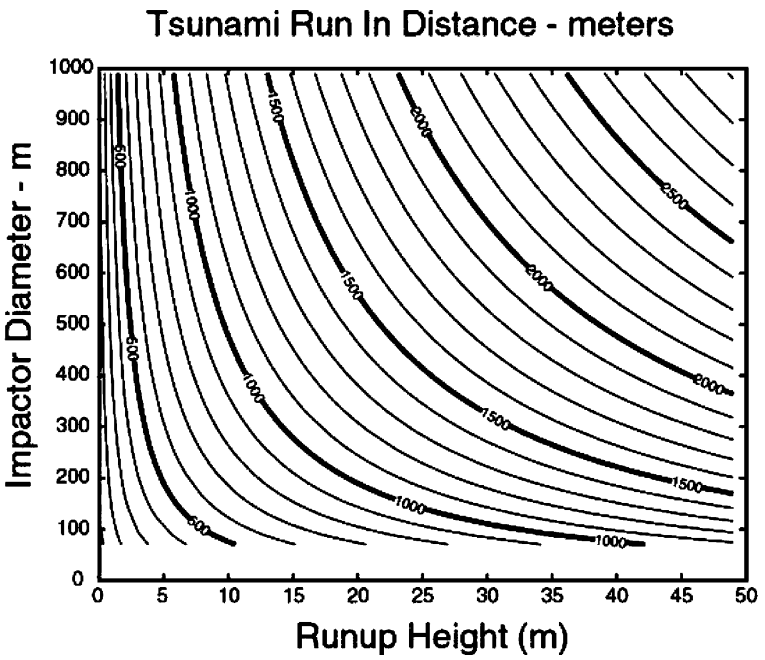

Figure 6. Contours of constant run-in distance $X(R,D_\mathrm{I})$ according to Equation (12).

$$\dot{N}_\mathrm{A}(R, D_\mathrm{I}) = N_\mathrm{R}(R, D_\mathrm{I}) R_\mathrm{w}(R, D_\mathrm{I}) \tag{14}$$

then, integrate (14) over all run-up and bolide diameters

$$\dot{N}_A = \iint\limits_{\text{allvalues}} \mathrm{d}R\mathrm{d}D_\mathrm{I} \dot{N}_A(R, D_\mathrm{I}). \tag{15}$$

On average, $\dot{N}_\mathrm{A} = 280$ people per year will be affected by impact tsunami given the generic assumptions so far. The rate of affected population can be broken down by run-up height

$$\dot{N}_\mathrm{A}(R) = \int_0^\infty \mathrm{d}D_\mathrm{I} \dot{N}_\mathrm{A}(R, D_\mathrm{I}) \tag{16}$$

(Figure 10, top left) or bolide diameter

$$\dot{N}_\mathrm{A}(D_\mathrm{I}) = \int_0^\infty \mathrm{d}R \dot{N}_\mathrm{A}(R, D_\mathrm{I}). \tag{17}$$

(Figure 10, top right). Due to atmospheric shielding, almost none of the risk associates with impactors smaller than 100 m in diameter. About 50% of the hazard derives from 100–300 m bolides, and more than 90% of the hazard derives from bodies smaller than the 1 km size that the Spaceguard Survey targets. About 50% (90%) of the affected population derives from wave run ups less than 11 m (33 m).

5. Corrections and Uncertainties to the Generic Model

The section above presented generic hazard rates based on the simplest assumptions. Now we attempt to correct biases and address uncertainties in the generic hazard model by means of "uncertainty multipliers" U. We

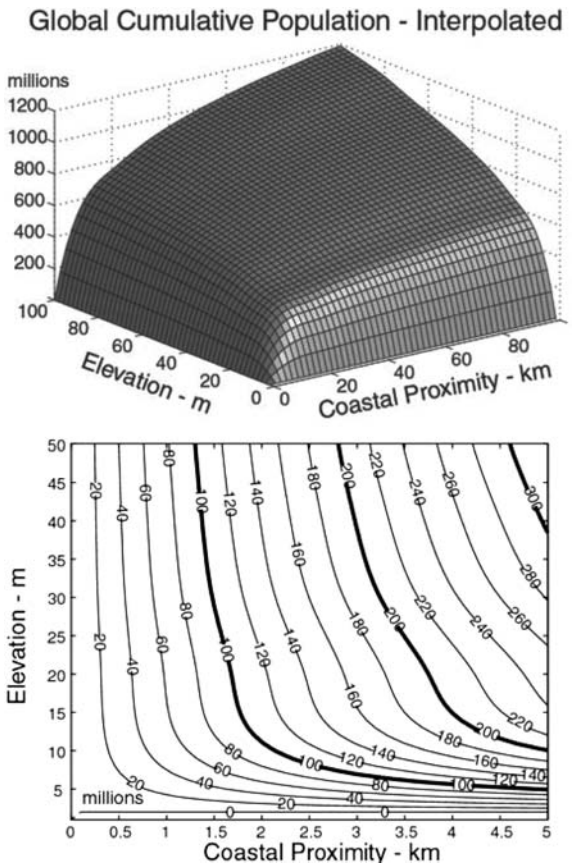

Figure 7. Cumulative global population $P_<(D, E)$ living within distance D of the coast and below elevation E (top); blow up of the front corner of the distribution (bottom).

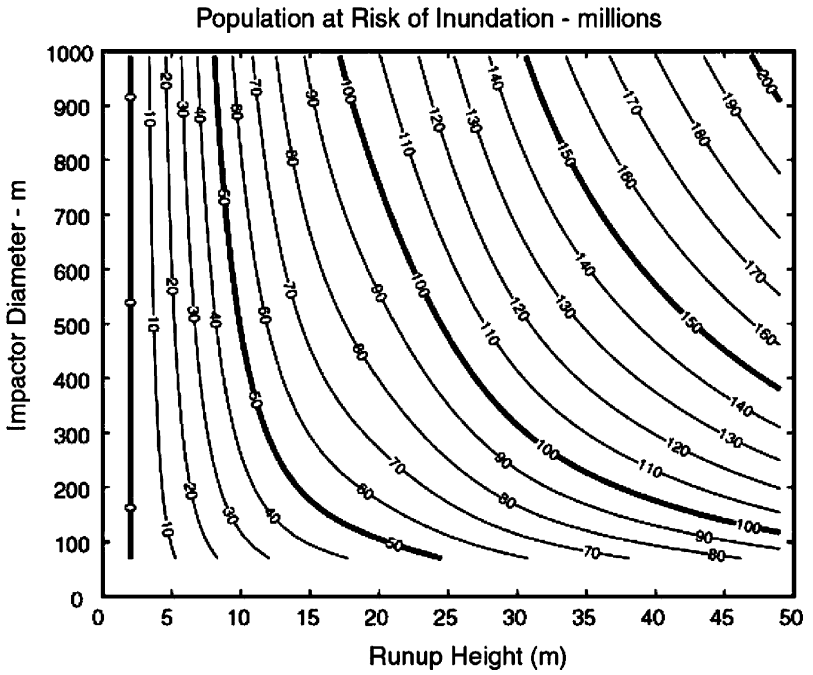

Figure 8. Contours of at-risk population $N_R(R,D_I)$ who live below a given run-up elevation and within the run-in distance.

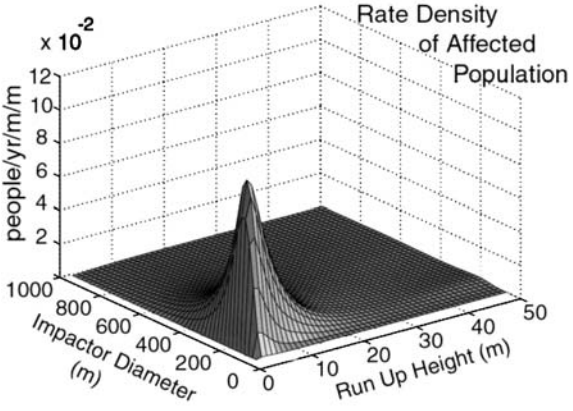

Figure 9. Rate density of affected population $\dot{N}_A(R, D_I)$.

intend the range of multipliers U to represent reasonable uncertainties in the mean effect of each process, not the event to event variability of the effects.

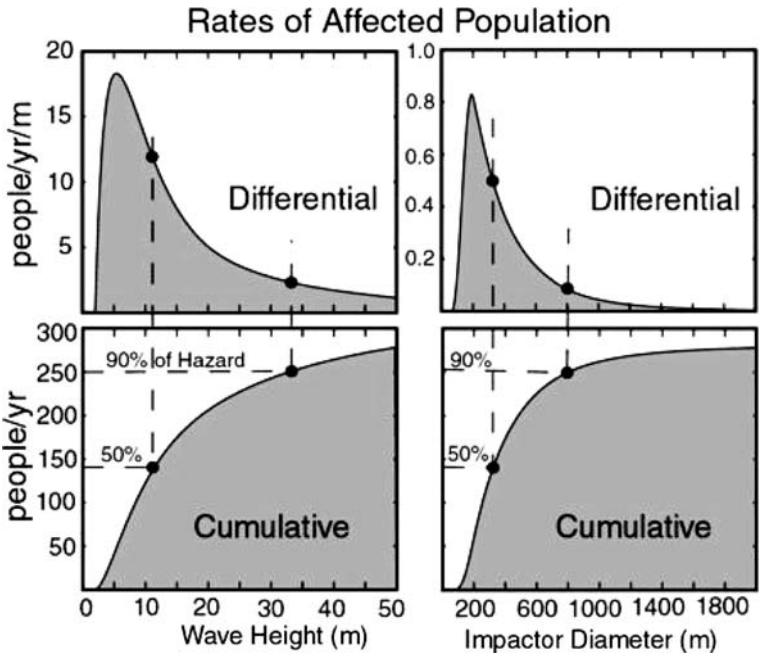

Figure 10. Affected population as a function of run-up height (left column) and impactor diameter (right column). Top and bottom rows show differential and cumulative rates.

5.1. TSUNAMI RATE UNCERTAINTY

(a) Asteroid population estimates based upon discovery and detection statistics (Brown *et al*., 2002) suggest that the population of 100–500 m NEAs may be depleted by a factor of two relative to the power law flux model (1). Also recent computer simulations by Bland and Artemieva (2003) suggest that atmospheric shielding may be more effective than modeled by (1b) ($U = 0.85 \pm 0.35$).

(b) Ward and Asphaug (2000) estimate that at a fixed impactor diameter, variations in kinetic energy and energy transfer efficiency contribute to a 20% uncertainty in the initial cavity depth (2) and diameter (3) ($U = 1.0 \pm 0.2$).

(c) Some detailed hydrodynamic simulations of marine impacts (Shuvalov, 2003; Gisler *et al*., 2003) hint that Ward and Asphaug's (2000) attenuation formula (4) may over-predict tsunami amplitudes for deep water impacts, possibly because their theory ignores dissipation and non-linear wave behaviors during cavity collapse. On the other hand, shallow water impact calculations by Shuvalov *et al*. (2002) hint that (4) may be low ($U = 0.85 \pm 0.35$).

5.2. BEACHING UNCERTAINTY

(a) For waves less than 15 m high, the interpolated population distribution (bottom, Figure 5) indicates that doubling or halving the assumed tsunami run-up elevation or run-in distance roughly doubles or halves the number of people exposed. We expect 50% uncertainty in run-up and run-in laws (7) and (12) with a comparable uncertainty in hazard ($U = 1.0 \pm 0.5$).
(b) In heavily developed areas, dissipation by structures reduces run-in (12). Moreover, large sheltered port cities present substantially reduced exposure and reach to the sea compared to the generic site. On the other hand, smoothing of digital coastlines causes harbor-protected populations to appear in Figure 5 at farther (hence safer) distances from the sea than in reality, so harbor protection is already partially accounted for ($U = 0.7 \pm 0.2$).
(c) Run-up estimates (7) agree well with experiments using solitary waves (Li, 2000). Frequency dispersion, however, spreads impact tsunami into long sequences of nearly periodic waves. When sets of periodic waves beach, wave pressure piles water onto the shore in a process called *set up*. Incoming tsunami ride on the *set up* pile and run-up higher and run-in farther than solitary waves. Wave setup might add 20–50% to the expected inundation. Recently, Melosh (2003) and Korycansky and Lynett (2005) revived a notion attributed to W.G. Van Dorn that offshore breaking of shoaling tsunami severely limits their potential run-up. The process, however, has yet to find experimental/observational support or to be quantified in a usable form like formula (7) ($U = 1.35 \pm 0.15$).

5.3. COASTAL POPULATION DISTRIBUTION

(a) The 10 km scale resolution of the underlying population data does not bear the 100 m scale interpolation of Figure 5 ($U = 1.0 \pm 0.3$).
(b) We assumed in Figure 1 that no one lives below 2 m elevation. Increasing (decreasing) the cleared elevation decreases (increases) the inundation rate by 10% for 1 m variation and 17% for 2 m of variation ($U = 0.95 \pm 0.15$).

If the uncertainty multipliers U, are independent random variables, then the mean of their product equals the product of their means and the variance of their product is

$$\sigma_U^2 = \prod \left(\int_0^\infty U^2 P[U] \mathrm{d}U \right) - \prod U_{\mathrm{mean}}^2; \tag{18}$$

Table I. Compilation of uncertainty multipliers on the generic hazard rate

	$U_{\min}$	U_{mean}	$U_{\max}$
Tsunamis rate			
(a) Impactor flux	0.5	0.85	1.2
(b) Initial cavity size	0.8	1.0	1.2
(c) Wave propagation	0.5	0.85	1.2
Beaching			
(a) Run-up and Run-in	0.5	1.0	1.5
(b) Harbor protection	0.5	0.7	0.9
(c) Wave setup	1.2	1.35	1.5
Coastal population			
(a) Interpolation	0.7	1.0	1.3
(b) Cleared elevation	0.8	0.95	1.1
Mean and 90% Confidence	0.21	0.65	1.35

where $P[U]$ is their probability density. If the multipliers have uniform probability over their range, then

$$\sigma_U^2 = \prod\left(\frac{U_{\max}^3 - U_{\min}^3}{3(U_{\max} - U_{\min})}\right) - \prod U_{\text{mean}}^2. \tag{19}$$

Given the long list of potential error sources, we find it no surprise that impact tsunami hazard estimates are fairly uncertain. The values listed in Table I indicate an overall standard deviation of, $\sigma_U = 0.36$ which is more than half of the mean $\overline{U} = 0.65$. Figure 11 plots the probability distribution of the product of the uncertainty multipliers. The range $0.21 < \overline{U} < 1.35$ covers 90% of events, so our best corrected rate affected population is $\dot{N}_A^{\text{corr}} = 182(+197/-123)/\text{y}$.

6. Other Hazard Implications

Tsunami from an impact 2000 km offshore take 3–5 h to beach depending on the width of the continental shelf lying on the wave's path. Even if NEA systems provide no warning beyond the first detection of a bolide in the atmosphere, the few hours of tsunami travel time might be adequate for evacuation of a coastal region a few kilometers wide. (Existing warning systems for earthquake-generated tsunami face comparable challenges and, as evidenced by the December 2004 Sumatra tsunami, the challenge has not always been met successfully.) For this reason, we do not interpret the rate of affected population given above as a fatality rate.

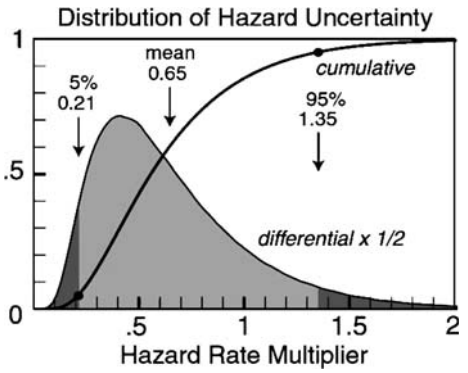

Figure 11. Probability distributions of uncertainty multiplier on the generic hazard rate.

While people might evacuate in short order, lacking weeks of advanced notice, most infrastructure would remain. Given infrastructure value versus elevation and distance from shore, we could compute affected infrastructure loss in the same fashion as affected population. Such shoreline specific calculations are in prospect, but in this article we suppose simply that each affected person ties to \$100,000 of infrastructure (Canavan, 1994). If so, the averaged annual economic loss rate from impact tsunami is \$18(+20/−12)M under the generic assumptions. Economic loss scales linearly with per capita infrastructure value, so impact tsunami presented on a high value coasts like California (Figure 1) would produce damages exceeding the stated generic loss multifold.

How might losses from impact tsunami distribute in time? From (17) the mean number of people affected per ocean impact of a bolide of size D_{I} to $D_{\mathrm{I}} + 1\mathrm{m}$ is

$$N_A^{\mathrm{event}}(D_{\mathrm{I}}) = \dot{N}_A^{\mathrm{corr}}(D_{\mathrm{I}})/f^{\mathrm{corr}}(D_{\mathrm{I}}) \tag{20}$$

with

$$f^{\mathrm{corr}}(D_{\mathrm{I}}) = 0.85\ (2/3)\frac{\partial f_{>}(D_{\mathrm{I}})}{\partial D_{\mathrm{I}}} \tag{21}$$

being 2/3 times the derivative of impact flux (1) corrected by its mean multiplier in Table I. N_A^{event} (D_{I}) and $f_{\mathrm{corr}}(D_{\mathrm{I}})$ are plotted in Figure 12. Per event, on average, tsunami from an ocean impact of the 200, 300 and 500 m and 1 km diameter bolides affect (Figure 12) 0.9, 2.5, 6.1 and 10.8 million people. At first, the number affected grows quickly with bolide size because larger and larger waves reach more and more coastline. Beyond $D_{\mathrm{I}} \sim$ 500 m however, the number affected per event

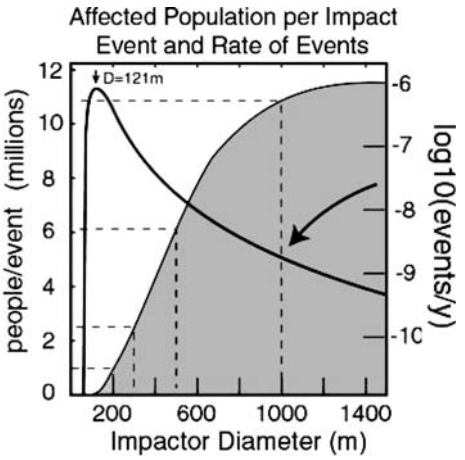

Figure 12. (gray region) Affected population per generic impact event of given diameter. This is Equation (20). (solid curve) Corrected ocean impact event rate versus impactor diameter. This is Equation (21). Atmospheric shielding creates the precipitous drop in impact rates at $D_I < 100$ m.

starts to saturate. Impactors of diameter greater than 500 m "bottom out" even in deep ocean, and by (4) no longer make increasingly larger waves. With an affected rate of hundreds per year, yet millions being affected per event, recurrence intervals must be long. Compared to other commonly considered losses, automobile accidents, say; the hazards from impact tsunami cluster tightly in time. To obtain the mean scenario, divide $\dot{N}_A^{\text{corr}}$ by the total corrected ocean impact rate $[0.85(2/3)\, f_>(60\,\text{m}) = 1.7 \times 10^{-4}/\text{y}]$. On average, one NEA will survive atmospheric transit and strike somewhere into Earth's oceans every 5880 years. In the mean generic scenario, the tsunami from the impact affects 1.1 million people and destroys \$110B of infrastructure. A generic impact of a 400 m diameter asteroid like 2004MN4 would destroy \$400B of infrastructure. For comparison, the estimated infrastructure loss due to the December 2004 Sumatra tsunami was \$10B (Cheesman, 2005).

7. Conclusions

We develop a framework to quantify human and economic losses from impact tsunami. Although the calculation involves some subjective assessments, the approach is straightforward and estimates can be refined simply when better information becomes available on impactor flux (1), tsunami

generation/attenuation (2–4), run-up (7), run-in (12) and population distribution (Figure 7). Ease of refinement is the primary merit of any quantitative hazard analysis.

Averaged over long term, we estimate that 182(+197/–123) people per year will be affected by tsunami from sub-2-km diameter NEA's with an average economic loss of \$18(+20/−12)M/y. About 90% of impact tsunami hazard finds origin in NEA's below the Spaceguard's nominal detection rolloff at 1 km size. About 50% finds origin below the 300 m size rolloff of LSST. Because of atmospheric shielding, almost none of the hazard derives from impactors with diameters less than 80 m.

Tsunami from asteroid impacts put 50 million of the Earth's population at risk. For this group, the $4 \times 10^{-6}(182y^{-1}/50$ million) annual likelihood of being affected by a sub-2 km asteroid impact somewhere into water is 400 times greater than the chance of being affected by a sub-2 km asteroid impact somewhere onto land and 8 times greater than the chance of being affected by km-plus asteroid impacts anywhere on Earth (NASA NEO SDT Report, 2003). That is, for the 50 million exposed coastal residents, the hazard from tsunami likely exceeds any other hazard posed by asteroid impacts.

If annualized tsunami losses alone formed a basis, the \$150M LSST would amortize in a decade of service. If however, the typical loss scenario displaces 1 million people and destroys \$100B of infrastructure at 6000 years intervals, then during its life the LSST has little chance of overlapping any impact event. Arguably its *short-term* mitigation value is nil. On the other hand, asteroid surveys primarily mitigate *long-term* impact hazard by reducing the population of undiscovered NEAs and by providing distant warning. Even if LSST is no longer operating when an impact occurs, tracking provided from it may hark of a strike centuries in the future, so its mitigation value transcends the system's life span.

Acknowledgements

Christopher Small generously provided the raw population data for this research. The analysis benefited from numerous discussions with Erik Asphaug, William Bottke, Alan Harris, Jay Melosh, David Morrison and Don Yeomans. Clark Chapman provided many helpful comments in review. The work of SRC was conducted at the Jet Propulsion Laboratory, California Institute of Technology, under a contract with the National Aeronautics and Space Administration.

Appendix

On the origin of run-up formula (7).

Consider an oscillatory tsunami wave train passing along a ray path from offshore position $\mathbf{r}_1$to near shore position $\mathbf{r}_2$. If wave amplitudes and still water depths at these locations are A_1, h_1 and A_2, h_2, respectively, linear water waves requires (Dingemans, 1997)

$$A_2^2 V_2 = \psi A_1^2 V_1 \tag{A1}$$

The V_1 and V_2 are frequency dependent group velocities and the parameter $\psi \leq 1$ accounts for energy that might lost along the path due to bottom friction, wave reflection, scattering and breaking. If at both locations the waves are assumed to be shallow water ones, then

$$V_1 = \sqrt{g(h_1 + A_1)}; \quad V_2 = \sqrt{g(h_2 + A_2)} \tag{A2}$$

If at both locations wave heights are much smaller than water depth, and energy losses are small, then (A1) reduces to Green's Law for long wave shoaling

$$A_2 = A_1 (h_1/h_2)^{1/4} \tag{A3}$$

Instead, let $h_1 \gg A_1$, but now at near shore point $\mathbf{r}_2$ let $A_2 \sim O(h_2)$. In this case, (A1) is

$$A_2 \sqrt[1/4]{h_2 + A_2} = \psi^{1/2} A_1 \sqrt[1/4]{h_1} \tag{A4}$$

When position $\mathbf{r}_2$ falls at the still water edge, water depth h_2 there vanishes and

$$A_2 = \psi^{2/5} [A_1^{4/5} h_1^{1/5}] \tag{A5}$$

Wave run-up height R is the parameter of interest. Run-up involves the exchange of kinetic energy of the wave at water edge to potential energy at peak height on shore, so run-up height exceeds the water edge amplitude, i.e.

$$R = \chi A_2 \text{ with } \chi > 1 \tag{A6}$$

Flume experiments (Li, 2000) suggest that wave height lost from frictional processes during final approach to the still water edge roughly cancel the superelevation of R relative to A_2 the wave height at water edge; that is $\chi \psi^{2/5} \approx 1$. Whence from (A5) and (A6)

$$R = A_1^{4/5} h_1^{1/5} \tag{A7}$$

comes our run-up formula (7).

References

Bland, P. A. and Artemieva, N. A.: 2003, Efficient disruption of small asteroids by Earth's atmosphere, *Nature* **424**, 288–291.

Brown, P., Spalding, R. E., ReVelle, D. O., Tagliaferri, E., and Worden, S. P.: 2002, The flux of small near-Earth objects colliding with the Earth, *Nature* **403**, 165–166.

Canavan, G. H.: 1994, Cost and benefit of near-Earth object detection and interception, In: T. Gehrels (ed), *Hazards Due to Comets and Asteroids*, Tucson: Univ. Arizona, pp. 1157–1190.

Cheesman, P.: 2005, The Asian Earthquake/Tsunami Disaster, An Insurance Perspective, Glencairn Re Limited, London. Available at http://www.glencairngroup.com/glen/images/glencairn_tsunami_report.pdf.

Dingemans, M. W.: 1997, *Water Wave Propagation over Uneven Bottoms, Part-1 Linear Wave Propagation*, World Scientific, Singapore.

Gisler, G. *et al.*: 2003, Two and three-dimensional simulations of asteroid ocean impacts. In: Results of the Workshop on Impact Cratering, LPI, Houston, TX.

Korycansky, D. G. and Lynett, P. J.: 2005, Offshore breaking of impact tsunami: The Van Dorn effect revisited. *Geophys. Res. Lett.* **32**, doi:10.1029/2004GL021918, L10608.

Lay, T., Kanamori, H., Ammon, C. J., Nettles, M., Ward, S.N., and others: 2005, The great Sumatra–Andaman earthquake of 26 December 2004. *Science* **308**, 1127–1133.

Li, Y.: 2000, Tsunamis: Non-breaking and breaking solitary wave run up, Ph.D. Thesis, Division of Engineering and Applied Science, California Institute of Technology.

Melsoh, H. J.: 2003, Impact-generated tsunamis: An over-rated hazard. *Lunar Planet. Sci. Conf.* **34**, Abstract 2013.

National Research Council: 2001, *Astronomy and Astrophysics in the New Millennium*, National Academy Press, Washington, DC. Available at http://nap.edu.

National Research Council: 2002, *New Frontiers in the Solar System: An Integrated Exploration Strategy*, National Academy Press, Washington, DC. Available at http://nap.edu.

NASA Near-Earth Object Science Definition Team Report: 2003, Study to Determine the Feasibility of Extending the Search for Near-Earth Objects to Smaller Limiting Diameters. Available at http://neo.jpl.nasa.gov.

Organization for Economic and Cooperative Development: 2003, *Final Report of the Workshop on Near Earth Objects: Risks, Policies and Actions, OECD Global Science Forum*, Frascati, Italy. Available at http://www.oecd.org.

Small, C., Gornitz, V., and Cohen, J.: 2000, Coastal hazards and the global distribution of human population, *Environ. Geosci.* **7**(1), 3–12.

Shuvalov, V. V., Dypvik, H., and Tsikalas, F.: 2002, Numerical simulations of the Mjolnir marine impact crater. *J. Geophys. Res.* **107**, E7, 10.1029/2001JE001698.

Shuvalov, V. V.: 2003, Numerical Modeling of the Eltanin Impact, LPSC, Abstract #1101.

Schweickart, R. L.: 2005, A Call to (Considered) Action, B612 Foundation Occasional Paper 0501, Tiburon, CA Available at http://www.b612foundation.org/papers/Call_for_Action.pdf.

Synolakis, C. E.: 1987, The runup of solitary waves, *J. Fluid Mech.* **185**, 523–545.

Ward, S. N. and Asphaug, E.: 2000, Asteroid Impact Tsunami: A Probabilistic Hazard Assessment, *Icarus* **145**, 64–78.

Ward, S. N. and Asphaug, E.: 2002, Impact Tsunami – Eltanin, *Deep-Sea Res. Part II* **46**(6), 1073–1079.

Ward, S. N. and Asphaug, E.: 2003, Asteroid impact tsunami of 16 March, 2880. *Geophys. J. Int.* **153**, F6–F10.